Diagn Interv Radiol 2026; DOI: 10.4274/dir.2026.264367

BREAST IMAGING

ORIGINAL ARTICLE

©Copyright 2026 Author(s) - Available online at dirjournal.org.
Content of this journal is licensed under a Creative Commons Attribution-NonCommercial 4.0 International License.

Contrast-enhanced mammography findings of idiopathic granulomatous mastitis: a retrospective analysis of seventy histopathologically proven cases

Dilşah Oral[1]
Ahmet Burak Kale[1]
Şebnem Örgüç[2]
Hanife Seda Mavili[3]
Teoman Coşkun[4]

[1]Manisa Demirci State Hospital, Clinic of Radiology, Manisa, Türkiye

[2]Manisa Celal Bayar University Faculty of Medicine, Department of Radiology, Manisa, Türkiye

[3]Manisa Celal Bayar University Faculty of Medicine, Department of Pathology, Manisa, Türkiye

[4]Manisa Celal Bayar University Faculty of Medicine, Department of General Surgery, Manisa, Türkiye

PURPOSE

This study aimed to characterize the contrast-enhanced mammography (CEM) findings of histopathologically confirmed idiopathic granulomatous mastitis (IGM), compare isolated mass and non-mass enhancement (NME) phenotypes, and explore the cumulative burden of malignancy-mimicking imaging features using an exploratory malignancy-mimicking feature score (MMFS).

METHODS

This retrospective single-center study included 70 women with histopathologically confirmed IGM who underwent CEM between 2021 and 2024. Imaging findings were reviewed in consensus by two breast radiologists according to the Breast Imaging Reporting and Data System Manual (2025 edition). Lesion morphology, enhancement characteristics, temporal enhancement patterns, conspicuity, and associated imaging findings were recorded. Patients with isolated mass lesions and isolated NMEs were compared. The MMFS was calculated from 12 predefined malignancy-mimicking CEM features, including moderate/high enhancement conspicuity, plateau/washout temporal enhancement patterns, suspicious mass morphology, segmental/linear NME distribution, and associated findings, such as skin thickening and axillary lymphadenopathy.

RESULTS

The mean patient age was 41.7 ± 8.7 years, and the mean lesion size was 57.3 ± 26.8 mm. NME was the predominant imaging presentation (55.7%), and 14.3% of patients demonstrated both mass and NMEs. Contrast enhancement was present in all lesions, with heterogeneous enhancement (44.3%), high enhancement conspicuity (44.3%), and axillary lymphadenopathy (47.1%) being common findings. Compared with isolated mass lesions, isolated NMEs were significantly larger (median = 70 vs. 50 mm; $P = 0.017$) and more frequently associated with skin thickening (46.2% vs. 9.5%; $P = 0.004$). The mean MMFS was 3.41 ± 1.66. All patients demonstrated at least one malignancy-mimicking imaging feature; 90.0% had two or more features, and 65.7% had three or more features.

CONCLUSION

IGM demonstrates a broad spectrum of CEM findings, including multiple imaging features conventionally considered suspicious for malignancy. NME is the predominant imaging phenotype and is associated with larger lesion size and more frequent skin thickening than isolated mass lesions. The high cumulative burden of malignancy-mimicking imaging features highlights the diagnostic challenge posed by IGM on CEM.

CLINICAL SIGNIFICANCE

IGM frequently mimics breast cancer on CEM because multiple suspicious imaging features often coexist within the same lesion. Familiarity with the CEM spectrum of IGM may facilitate the appropriate interpretation of suspicious findings and contribute to informed patient management.

KEYWORDS

Breast imaging, contrast-enhanced mammography, idiopathic granulomatous mastitis, malignancy-mimicking features, non-mass enhancement

Handling editor: Gamze Durhan

Corresponding author: Dilşah Oral

E-mail: dilsahoral@gmail.com

Received 04 August 2026; revision requested 28 August 2026; last revision requested 27 September 2026; accepted 15 October 2026.

Epub: 10.11.2026

DOI: 10.4274/dir.2026.264367

You may cite this article as: Oral D, Kale AB, Örgüç Ş, Mavili HS, Coşkun T. Contrast-enhanced mammography findings of idiopathic granulomatous mastitis: a retrospective analysis of seventy histopathologically proven cases. *Diagn Interv Radiol*. 10 November 2026 DOI: 10.4274/dir.2026.264367 [Epub Ahead of Print].

Idiopathic granulomatous mastitis (IGM) is a chronic benign inflammatory disorder of the breast with an incompletely understood etiology. It predominantly affects parous women of reproductive age and typically presents with a palpable breast mass, pain, erythema, nipple retraction, abscess formation, or fistulous tracts. Despite its benign nature, the clinical presentation of IGM frequently overlaps with that of breast cancer, leading to diagnostic uncertainty and concern for malignancy and often necessitating histopathological confirmation.[1-3] Multiple etiological factors have been implicated in its development, such as hormonal dysregulation, autoimmune reactions, unidentified infectious agents, smoking, and α1-antitrypsin deficiency.[4] IGM is often a self-limiting condition that may be managed conservatively with corticosteroids or other immunomodulatory agents. However, surgical excision remains an effective treatment option in patients with suspected abscess formation or when corticosteroid therapy is contraindicated.[5] Recent evidence suggests that topical and intralesional corticosteroid administration provides efficacy comparable with that of oral corticosteroid therapy, leading to its increasing adoption as a first-line treatment approach.[6]

Imaging evaluation of IGM is particularly challenging because its radiologic manifestations are highly variable and often nonspecific. On mammography, findings may include focal asymmetry, irregular masses, architectural distortion, or skin thickening. Ultrasonography commonly demonstrates irregular hypoechoic masses, tubular extensions, abscesses, and sinus tracts. Doppler ultrasonography may reveal increased vascularity within the lesion and surrounding breast tissue. Magnetic resonance imaging (MRI) has also been reported to show suspicious features such as heterogeneous or rim enhancement, non-mass enhancement (NME), and kinetic patterns that may mimic malignancy. Consequently, IGM is frequently assigned suspicious imaging assessments despite representing a benign inflammatory process.[2,7,8]

Main points

- Idiopathic granulomatous mastitis (IGM) demonstrates a broad spectrum of malignancy-mimicking findings on contrast-enhanced mammography (CEM).
- Non-mass enhancement is the predominant CEM presentation of IGM and is associated with larger lesion size and more frequent skin thickening than isolated mass lesions.
- Multiple malignancy-mimicking imaging features frequently coexist within the same lesion, highlighting the diagnostic challenge of IGM on CEM.
- The proposed malignancy-mimicking feature score provides an exploratory descriptive index of the cumulative burden of malignancy-mimicking CEM features in IGM.
- Familiarity with the CEM spectrum of IGM may facilitate appropriate interpretation of its malignancy-mimicking imaging features within the clinical context.

Contrast-enhanced mammography (CEM) has emerged as a valuable breast imaging modality by combining morphologic information from low-energy mammographic images with functional assessment of lesion vascularity. Owing to its high sensitivity for lesion detection and characterization, CEM is increasingly incorporated into the diagnostic evaluation of suspicious breast findings.[9-11] However, inflammatory breast diseases may also demonstrate contrast enhancement, limiting the specificity of the technique. Although the CEM appearance of breast malignancies has been extensively investigated, data regarding the imaging characteristics of IGM on CEM remain limited. Existing imaging literature on IGM has largely focused on mammography, ultrasonography, and MRI. Consequently, the characteristic findings and potential diagnostic role of CEM in this disease remain undefined. Therefore, the aim of this study is to characterize the CEM findings of histopathologically confirmed IGM, compare isolated mass and NME phenotypes, and explore the cumulative burden of malignancy-mimicking CEM features using an exploratory descriptive malignancy-mimicking feature score (MMFS).

Methods

This retrospective study was approved by the Manisa Celal Bayar University Faculty of Medicine Clinical Research Ethics Committee (approval number: E-85252386-050.04.04-503989, date: 06.03.2023). Owing to the retrospective nature of the study, the ethics committee waived the requirement for written informed consent. A total of 927 consecutive patients who underwent CEM between 2021 and 2024 because of clinical suspicion of breast cancer or suspicious findings on other breast imaging modalities were retrospectively evaluated (Figure 1). The inclusion criteria were as follows: (1) histopathologically confirmed granulomatous mastitis, (2) absence of an identifiable underlying cause, consistent with IGM, and (3) availability of CEM images of sufficient quality for imaging assessment. Patients with granulomatous mastitis attributable to a specific underlying cause, those without histopathological confirmation, and those with incomplete or inadequate CEM examinations were excluded.

Contrast-enhanced mammography acquisition protocol

All CEM examinations were performed using a dual-energy digital mammography system (Senographe Pristina, GE Medical Systems SCS, Buc, France). A low-osmolar, nonionic contrast agent was administered at a dose of 1.5 mL/kg (maximum 100 mL) using an automatic injector at a rate of 3 mL/s. CEM imaging was initiated 1.5–2 minutes after contrast injection. The CEM acquisition protocol was standardized across the study cohort. Craniocaudal and mediolateral oblique (MLO) images were acquired bilaterally, starting with the target breast. An additional delayed MLO image of the affected breast was obtained at approximately 8 minutes after contrast administration, following acquisition of the MLO image of the contralateral breast for all patients. The total examination time was approximately 8–9 minutes, depending on patient compliance. Low-energy images were obtained using tube voltages ranging from 28 to 32 kVp, whereas high-energy images were acquired at 45–49 kVp. The system automatically selected the appropriate filtration material and exposure parameters. Recombined images were subsequently generated by the system using the low- and high-energy image datasets.

Image analysis

All CEM examinations were reviewed in consensus by two breast radiologists with 6 and 35 years of experience, respectively. During this consensus review, the radiologists evaluated the CEM images exclusively; ultrasonography or other imaging modalities were not retrospectively re-evaluated. All CEM imaging variables, including those used to calculate the MMFS, were determined solely from this retrospective consensus CEM review. As image interpretation was performed by consensus rather than independently, interobserver agreement was not assessed. The CEM image evaluation was conducted according to the American College of Radiology Breast Imaging Reporting and Data System (BI-RADS®) Manual (2025 edition).

The following variables were recorded for each patient: age, BI-RADS category from the final clinical reports, lesion size measured in the longest single-plane dimension on re-

combined images, background parenchymal enhancement (BPE), lesion type (mass, NME, or both), mass shape (oval, round, lobulated, or irregular), mass margins (circumscribed, indistinct, or spiculated), NME distribution (diffuse, regional, focal, linear, or segmental), and enhancement patterns (homogeneous, heterogeneous, rim, or clumped). The BI-RADS categories were not reassigned by the reviewing radiologists during the retrospective CEM evaluation. Instead, the final BI-RADS categories were extracted directly from the original clinical reports, in which BI-RADS assessment had been based on the combined evaluation of CEM and ultrasonography findings in routine clinical practice.

Lesion conspicuity was assessed on recombined CEM images and categorized as low, moderate, or high according to the degree of contrast enhancement relative to the surrounding breast parenchyma. Lesion visibility on low-energy images was also assessed and classified as none/low, moderate, or high. For temporal enhancement assessment, the change in lesion enhancement intensity relative to the background between the early and delayed images was visually evaluated. Based on this temporal change, enhancement was classified as persistent, plateau, or washout. No quantitative signal-intensity thresholds were applied; classification was based on visual comparison of enhancement between the available early and delayed acquisitions. In addition, associated imaging findings, including nipple retraction, skin retraction, skin thickening, fistula formation, and axillary lymphadenopathy, were documented. For descriptive analysis, lesions were categorized as isolated mass, isolated NME, or combined mass + NME. Mass-specific morphological features, including shape and margin, were evaluated in all lesions containing a mass component (n = 31), including combined mass + NME lesions. NME distribution was evaluated in patients with isolated NME (n = 39). For the direct comparison of isolated mass and isolated NME phenotypes, patients with combined mass + NME (n = 10) were excluded to ensure mutually exclusive groups. Lesion size and rim enhancement were also compared between patients with and without fistula formation.

The MMFS was calculated using 12 predefined malignancy-mimicking CEM features. These included moderate or high conspicuity on recombined images, a plateau or washout enhancement pattern, an irregular mass shape, an indistinct or spiculated mass margin, heterogeneous enhancement, rim enhancement, segmental or linear NME distribution, clumped enhancement, skin thickening, skin retraction, nipple retraction, and axillary lymphadenopathy. Each feature was assigned 1 point to provide a simple descriptive measure of the cumulative burden of malignancy-mimicking findings; equal weighting was not intended to imply equivalent diagnostic or predictive significance of the individual features.

Statistical analysis

Statistical analyses were performed using IBM SPSS Statistics (Version 27.0; IBM Corp., Armonk, NY, USA). Continuous variables were assessed for normality and are presented as mean ± standard deviation or median [interquartile range (IQR)], as appropriate, and categorical variables are presented as frequencies and percentages. Comparisons between patients with isolated mass and isolated NME were performed using the independent-samples t-test or Mann–Whitney U test for continuous variables and the χ^2 test or Fisher's exact test for categorical variables, as appropriate. The association between rim enhancement and fistula formation was evaluated using Fisher's exact test, and lesion size was compared between patients with and without fistula formation using the Mann–Whitney U test. All statistical tests were two-sided, and a P value of < 0.05 was considered statistically significant.

Results

A total of 70 women with histopathologically confirmed IGM were included in the study. The mean age was 41.7 ± 8.7 years (range: 24–65 years). The mean lesion size was 57.3 ± 26.8 mm (range: 12–130 mm). Minimal BPE was the most common pattern, observed in 48 of 70 patients (68.5%). NME was observed in 49 patients (70.0%) (Figures 2, 3), including 10 patients who also demonstrated an associated mass lesion (Figures 4, 5). Mass lesions were identified in 31 patients (44.3%) (Figure 6), with 21 patients showing a mass without accompanying NME. Among mass lesions, lobulated (32.3%) and oval (29.0%) shapes were the most common morphologies. Indistinct or spiculated margins were identified in 8 patients (25.8%). Contrast enhancement was observed in all lesions, with no cases showing complete absence of enhancement. Heterogeneous enhancement was the predominant enhancement pattern (44.3%), followed by rim enhancement (22.9%). High conspicuity on recombined images was observed in 31 patients (44.3%). Associated findings included axillary lymphadenopathy in 33 patients (47.1%), skin thickening in 23 (32.9%), nipple retraction in 20 (28.6%), skin retraction in 11 (15.7%), and fistula formation in 12 (17.1%). Persistent enhancement was the most common pattern, occurring in 48 patients (68.6%) (Table 1).

Fistula formation was observed in 4 of 16 patients (25.0%) with rim enhancement and in 8 of 54 patients (14.8%) without rim enhancement. Although fistulas were numerically more frequent among lesions demonstrating rim enhancement, the association did not reach statistical significance (Fisher's exact test, $P = 0.45$). Lesion size did not differ significantly between patients with and without fistula formation. The median lesion size was 48.0 mm (IQR: 39.5–62.5 mm) in the fistula group and 60.0 mm (IQR: 37.0–76.5 mm) in the non-fistula group ($P = 0.651$).

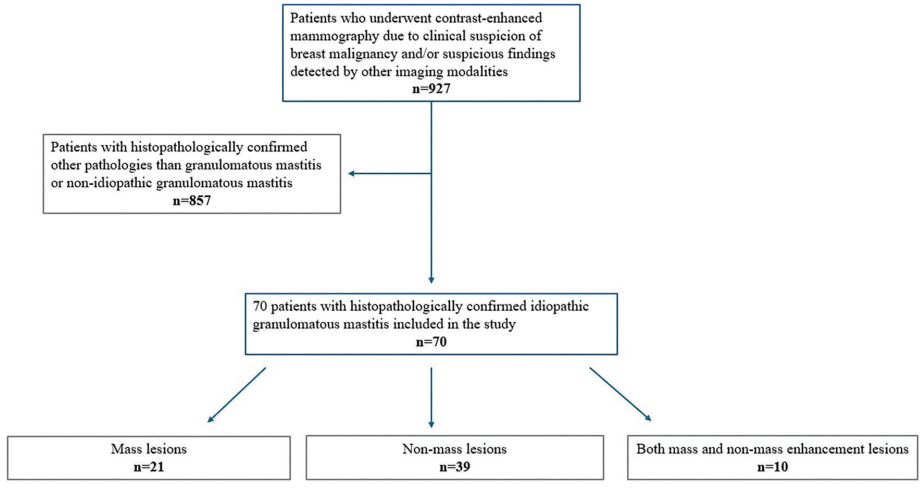


Figure 1. Flowchart of the study.

Patients with isolated mass lesions (n = 21) and isolated NME (n = 39) were compared (Table 2). Isolated NME lesions were significantly larger than isolated mass lesions (median size, 70 mm vs. 50 mm; $P = 0.017$) and were more frequently associated with skin thickening (46.2% vs. 9.5%; $P = 0.004$). No significant differences were observed regarding age, BPE, conspicuity, low-energy image visibility, temporal enhancement pattern, or other associated imaging findings (all $P > 0.05$).

The frequencies of individual malignancy-mimicking imaging findings are summarized in Table 3. Moderate or high conspicuity on recombined images (62.9%), axillary lymphadenopathy (47.1%), and heterogeneous enhancement (44.3%) were the most frequently encountered malignancy-mimicking features. The mean MMFS was 3.41 ± 1.66, with a median score of 3 (IQR: 2–5; range: 1–8). All patients demonstrated at least one malignancy-mimicking imaging feature. Sixty-three patients (90.0%) exhibited two or more features, and 46 (65.7%) exhibited three or more features. The most frequent MMFS values were 2 and 3, each observed in 17 patients (24.3%), followed by a score of 5 in 12 patients (17.1%). Four patients (5.7%) had MMFS values of ≥ 7 (Table 4).

Discussion

The present study demonstrates that IGM exhibits a heterogeneous spectrum of CEM appearances, with multiple imaging features conventionally associated with breast malignancy frequently coexisting within the same lesion.[12,13] NME emerged as the predominant imaging phenotype and was associated with larger lesion size and more frequent skin thickening than isolated mass lesions, suggesting a more extensive pattern of inflammatory involvement. Another notable finding was the discrepancy between lesion visibility on low-energy images and contrast enhancement on recombined images. Although approximately one-third of lesions showed none or low visibility on low-energy images, all lesions demonstrated enhancement on recombined images. This finding is particularly relevant given that previous studies have reported normal or subtle mammographic findings in a subset of patients with IGM.[14] Finally, the frequent coexistence of malignancy-mimicking features, reflected by their cumulative burden in the MMFS, further illustrates the substantial imaging overlap between IGM and breast malignancy. Collectively, these findings expand the limited literature on the CEM appearance

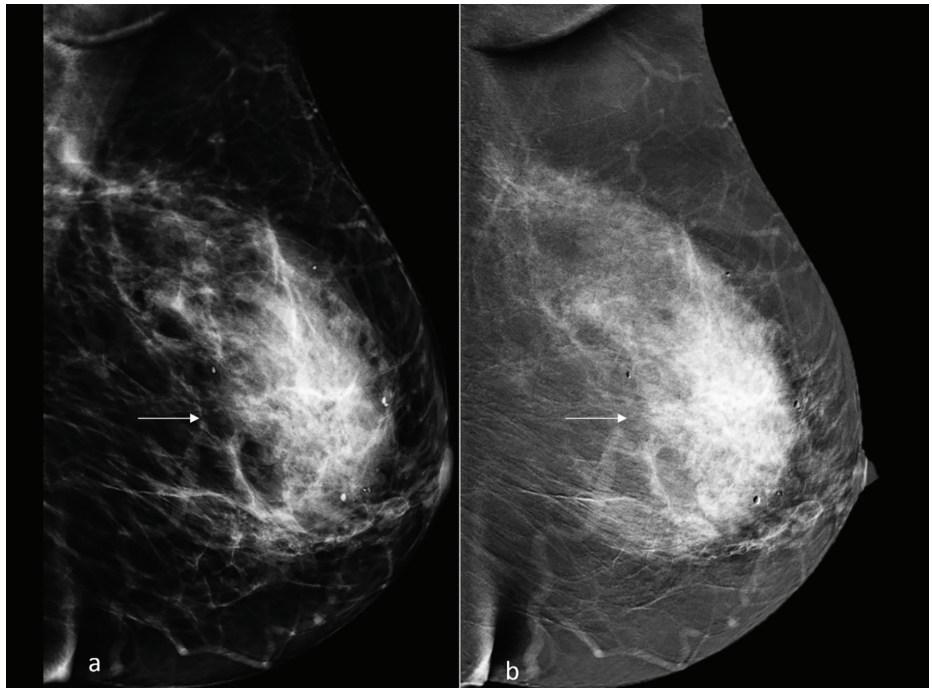


Figure 2. A 38-year-old woman with idiopathic granulomatous mastitis. **(a)** Low-energy image demonstrates diffuse increased breast opacity (arrow). **(b)** The corresponding recombined image demonstrates diffuse, high-conspicuity heterogeneous non-mass enhancement involving the breast (arrow).

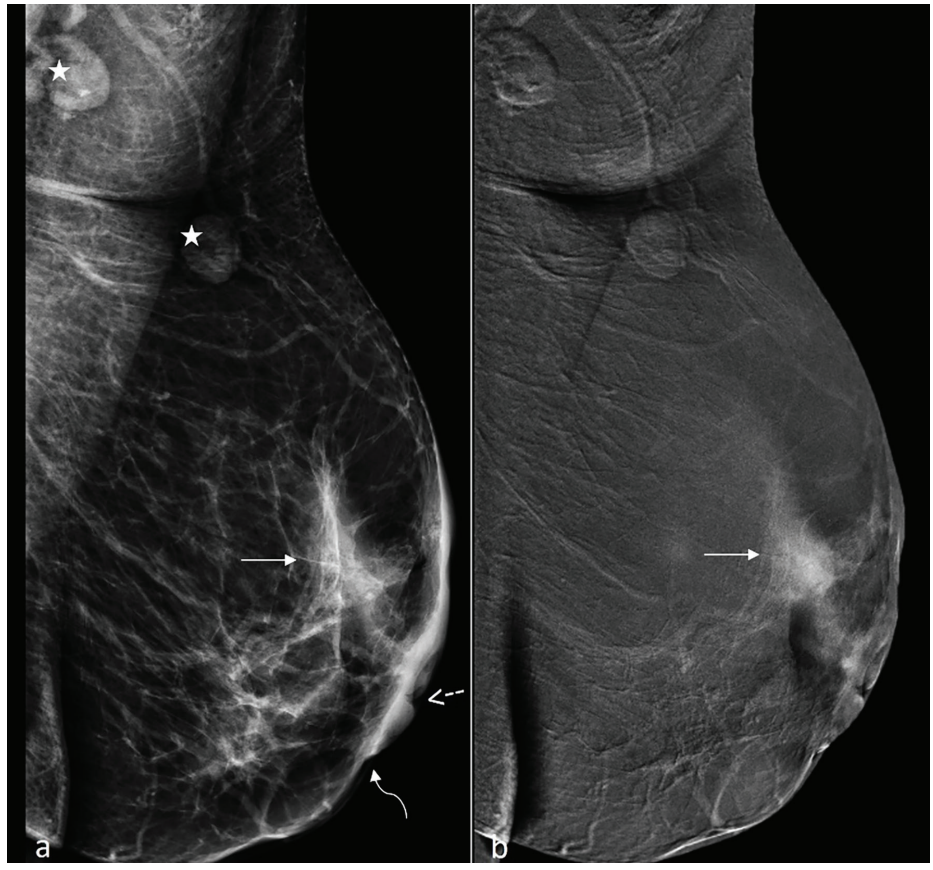


Figure 3. A 51-year-old woman with idiopathic granulomatous mastitis. **(a)** Low-energy image demonstrates increased opacity in the upper breast (arrow), associated with skin thickening and skin retraction (curved arrow), nipple retraction (dashed arrow), and axillary lymphadenopathy (asterisk). **(b)** The corresponding recombined image demonstrates high-conspicuity, segmental, heterogeneous non-mass enhancement in the upper breast (arrow).

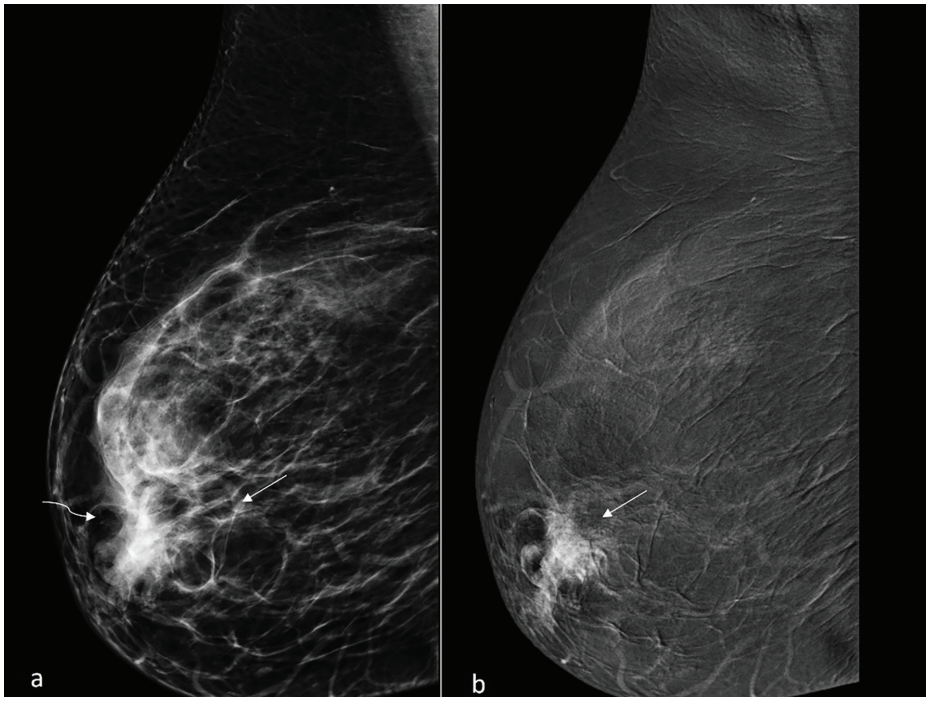


Figure 4. A 44-year-old woman with idiopathic granulomatous mastitis. **(a)** Low-energy image demonstrates increased retroareolar opacity (arrow) associated with skin thickening and nipple retraction (curved arrow). **(b)** The corresponding recombined image demonstrates an irregular mass with indistinct margins and high-conspicuity, heterogeneous enhancement, with associated focal non-mass enhancement in the retroareolar region (arrow).

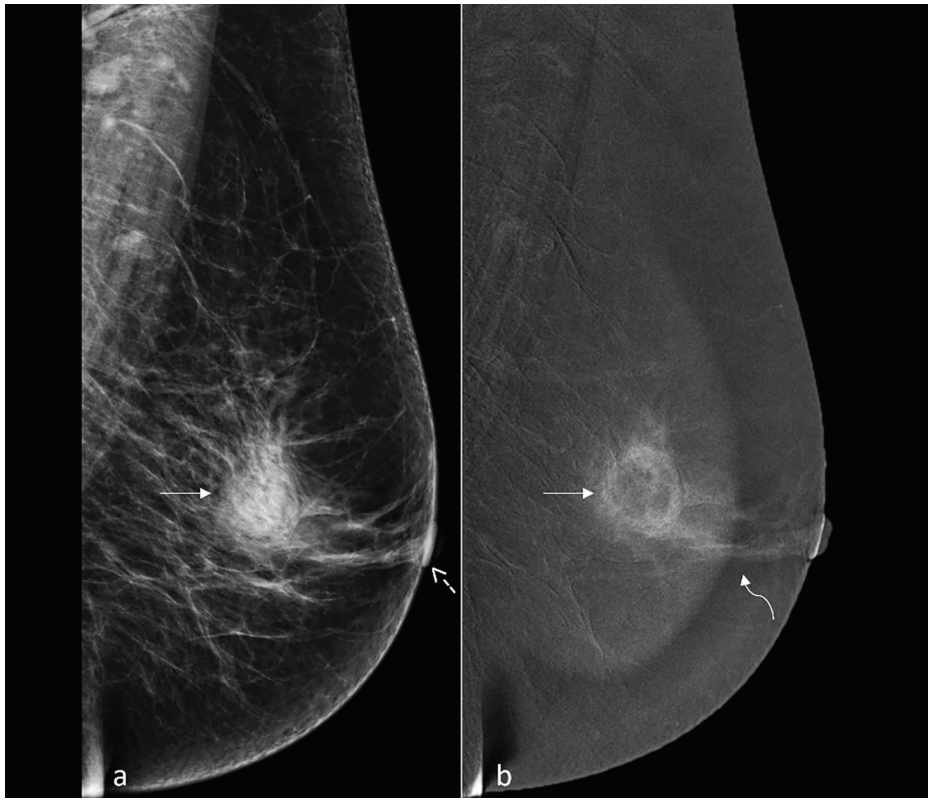


Figure 5. A 65-year-old woman with idiopathic granulomatous mastitis. **(a)** Low-energy image demonstrates a retroareolar opacity (arrow) with mild nipple retraction (dashed arrow). **(b)** The corresponding recombined image demonstrates a high-conspicuity round mass with rim enhancement (arrow). Enhancement extends from the mass toward the nipple as a contiguous non-mass enhancement component (curved arrow).

of IGM and provide a framework for interpreting its heterogeneous and potentially misleading imaging manifestations.

Previous studies have shown that IGM commonly manifests as focal asymmetry on mammography, irregular hypoechoic masses with increased vascularity and fluid collections on ultrasound, and irregular enhancing lesions with associated NME on MRI.[14-16] MRI studies have demonstrated that IGM may present as either mass lesions, NME, or a combination of both.[17,18] NME was the predominant imaging presentation in this cohort, with segmental distribution being the most frequent pattern consistent with previous MRI studies.[17,19-21] Because segmental enhancement on CEM is generally considered a suspicious feature associated with breast carcinoma,[22] its presence in IGM may further contribute to the malignancy-mimicking appearance of the disease. Consistent with previous studies, most mass lesions in this cohort exhibited circumscribed margins despite their suspicious enhancement characteristics.[17]

In the present study, isolated NME lesions were significantly larger and more frequently associated with skin thickening than isolated mass lesions. These findings suggest that different imaging phenotypes of IGM may reflect distinct patterns of inflammatory involvement on CEM. The larger size of isolated NME lesions is not unexpected, as NME often represents diffuse inflammatory infiltration along the ductal-lobular system and surrounding parenchyma rather than a localized inflammatory focus. Similarly, the significantly higher prevalence of skin thickening in the NME group may indicate more extensive inflammatory involvement beyond the primary lesion, resulting in secondary skin involvement. Although differences in fistula formation, nipple retraction, and skin retraction did not reach statistical significance, these findings were also numerically more common in the NME group.

In contrast, plateau or washout temporal enhancement patterns were more frequent in isolated mass lesions than in isolated NME lesions (52.4% vs. 25.7%); however, the overall distribution of temporal enhancement patterns did not differ significantly between the groups ($P = 0.100$). Although this finding should be interpreted cautiously, the relatively higher frequency of plateau or washout patterns in mass lesions may contribute to the malignancy-mimicking appearance of focal IGM on CEM. Nevertheless, conspicuity, BPE, and other associated imaging findings

were largely comparable between the two groups, underscoring the substantial overlap in CEM appearances across different manifestations of IGM.

As in previous studies, temporal enhancement patterns demonstrate considerable variability, further supporting the notion that IGM may mimic breast malignancy not only morphologically but also functionally.[14,15] MRI studies have consistently demonstrated a high prevalence of plateau and washout enhancement patterns in patients with IGM.[17,23] This proportion was only 31.4% in our CEM cohort. This discrepancy may reflect inherent differences between MRI and CEM in the assessment of contrast enhancement kinetics, as CEM provides a simplified evaluation based on limited early and delayed acquisitions rather than continuous dynamic imaging. Therefore, direct comparisons between temporal enhancement patterns observed on CEM and kinetic patterns derived from dynamic contrast-enhanced MRI should be interpreted cautiously.

Several imaging features on CEM have been associated with breast malignancy, including linear or segmental NME, clumped enhancement, moderate or high enhancement conspicuity, nipple retraction, skin involvement, axillary lymphadenopathy, irregular mass shape, and indistinct or spiculated margins.[24-27] These descriptors were therefore incorporated into the exploratory MMFS evaluated in the present study. Abscess and fistula formation have been reported as imaging findings that may favor the diagnosis of IGM over invasive breast carcinoma.[19] Nevertheless, on CEM, rim enhancement alone may not reliably distinguish inflammatory abscesses from necrotic malignancies, as both entities may exhibit this enhancement pattern. Accordingly, rim enhancement was considered a malignancy-mimicking imaging feature in the MMFS. Plateau and washout temporal enhancement were also included in the MMFS based on evidence from previous MRI and CEM studies demonstrating their association with breast malignancy.[28-31]

One of the most notable findings of this study was the high cumulative burden of malignancy-mimicking imaging features among patients with IGM. Although individual suspicious findings have previously been described in IGM, our results demonstrate that these features frequently coexist within the same lesion. All patients exhibited at least one malignancy-mimicking imaging feature, 90% demonstrated two or more features, and

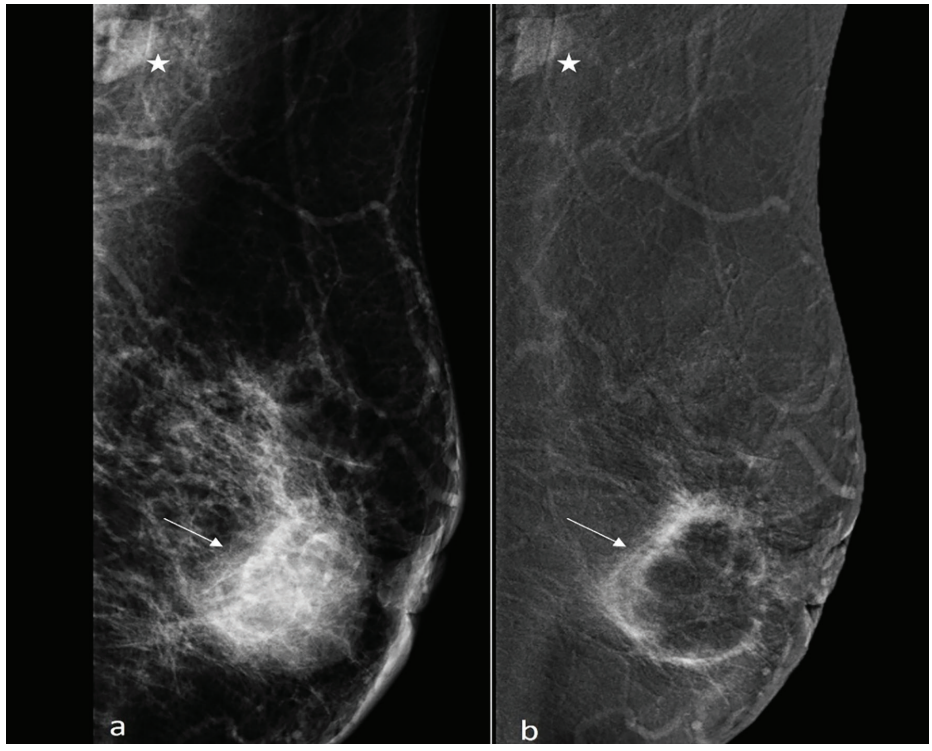


Figure 6. A 45-year-old woman with idiopathic granulomatous mastitis. **(a)** Low-energy image demonstrates a retroareolar opacity (arrow). **(b)** The corresponding recombined image demonstrates an oval, high-conspicuity mass with rim enhancement (arrow). Axillary lymphadenopathy with cortical thickening is also visible (asterisk).

Table 1. Patient characteristics and contrast-enhanced mammography findings of idiopathic granulomatous mastitis (n = 70)

Characteristic	Value
Age (years)	41.7 ± 8.7
Lesion size (mm)	57.3 ± 26.8
Final Breast Imaging Reporting and Data System category from the original clinical reports*	
4A	52 (74.3)
4B	5 (7.1)
4C	11 (15.7)
5	2 (2.9)
Background parenchymal enhancement	
Minimal	48 (68.5)
Moderate	16 (22.9)
Marked	6 (8.6)
Lesion type	
Mass	21 (30)
NME	39 (55.7)
Mass + NME	10 (14.3)
Mass shape (n = 31)	
Oval	9 (29.0)
Round	5 (16.1)
Lobulated	10 (32.3)
Irregular	7 (22.6)
Mass margin (n = 31)	
Circumscribed	23 (74.2)
Indistinct	5 (16.1)

Table 1. Continued

Characteristic	Value
Spiculated	3 (9.7)
NME distribution (n = 39)	
Focal	3 (7.7)
Linear	1 (2.6)
Segmental	17 (43.6)
Regional	11 (28.2)
Diffuse	7 (17.9)
Internal enhancement pattern	
Homogeneous	18 (25.7)
Heterogeneous	31 (44.3)
Clumped	5 (7.1)
Rim	16 (22.9)
Conspicuity on recombined images	
Low	26 (37.1)
Moderate	13 (18.6)
High	31 (44.3)
Visibility on low-energy images	
None/low	24 (34.3)
Moderate	10 (14.3)
High	36 (51.4)
Temporal enhancement pattern	
Persistent	48 (68.6)
Plateau	19 (27.1)
Washout	3 (4.3)
Associated findings	
Axillary lymphadenopathy	33 (47.1)
Skin thickening	23 (32.9)
Nipple retraction	20 (28.6)
Fistula formation	12 (17.1)
Skin retraction	11 (15.7)

Data are presented as mean ± standard deviation or n (%), as appropriate.
Mass-specific morphological features were evaluated in all lesions containing a mass component (n = 31). Non-mass enhancement distribution was evaluated in patients with isolated non-mass enhancement (NME) (n = 39).
*The Breast Imaging Reporting and Data System (BI-RADS) categories represent the final clinical assessment extracted from the original clinical reports and were based on the combined evaluation of contrast-enhanced mammography (CEM) and ultrasonography findings; they were not retrospectively assigned on the basis of CEM alone and should not be interpreted as CEM-specific BI-RADS assessments.

nearly two-thirds exhibited at least three features. Furthermore, 40% of patients showed four or more suspicious imaging characteristics. These findings illustrate the substantial overlap between the CEM appearance of IGM and imaging features conventionally associated with breast malignancy. The frequent occurrence of enhancement-related suspicious findings in our cohort is also biologically plausible. Granulomatous inflammation is characterized by increased vascular permeability, inflammatory hyperemia, and disruption of normal tissue architecture, all of which may contribute to contrast enhancement patterns that resemble those of malignant tumors. However, the present study did not include a malignant control group and therefore cannot determine the discriminatory value of these enhancement characteristics or of the MMFS. Rather than representing an isolated imaging pitfall, IGM appears to constitute a constellation of overlapping suspicious imaging findings, collectively contributing to its well-recognized tendency to mimic breast cancer on CEM.

This study has several limitations. First, its retrospective, single-center design may limit the generalizability of the findings. Second, although this represents one of the largest reported cohorts of histopathologically confirmed IGM evaluated with CEM, the sample size remains relatively limited because of the rarity of the disease. Third, image interpretation was performed by consensus rather than independently; therefore, inter-observer agreement for individual CEM features and the MMFS could not be assessed. Future studies incorporating independent reader assessments are needed to establish the reproducibility of these findings across observers. Fourth, the requirement for histopathological confirmation may have introduced selection bias toward more suspicious lesions, as patients with clinically or radiologically typical benign inflammatory findings are less likely to undergo biopsy. Consequently, the high prevalence and cumulative burden of malignancy-mimicking features observed in our cohort may not fully represent the broader spectrum of IGM, and the MMFS distribution should therefore be interpreted within the context of this selected population. Fifth, the absence of a histopathologically confirmed malignant control group precluded assessment of the discriminatory performance of individual CEM features or the MMFS in differentiating IGM from breast malignancy. Sixth, although lesion size was assessed by measuring the maximum lesion dimension on recombined images, the extent of enhancement relative to the corresponding abnormality on low-energy images was not systematically recorded. Finally, temporal enhancement patterns on CEM were derived from early and delayed acquisitions rather than continuous dynamic imaging and therefore should not be considered directly comparable with kinetic assessments obtained with dynamic contrast-enhanced MRI.

Taken together, these findings demonstrate that IGM may exhibit multiple malignancy-mimicking features on CEM, often coexisting within the same lesion. Awareness of this spectrum may facilitate the appropriate interpretation of suspicious CEM findings in the clinical context. The MMFS should be regarded as an exploratory descriptive measure of the cumulative burden of malignancy-mimicking features rather than a diagnostic or discriminatory tool. Future prospective, multicenter studies incorporating histopathologically confirmed malignant control

Table 2. Comparison of patients with isolated mass lesions and isolated non-mass enhancement

Variable	Isolated mass (n = 21)	Isolated NME (n = 39)	*P* value
Age, years	41 (37–50)	41 (36.5–48.5)	0.901
Lesion size, mm	50 (30–70)	70 (40–87.5)	**0.017**
Moderate/marked background parenchymal enhancement	6 (28.6%)	13 (33.3%)	0.778
Low conspicuity on recombined images	8 (38.1%)	15 (38.5%)	
Moderate conspicuity on recombined images	2 (9.5%)	5 (12.8%)	
High conspicuity on recombined images	11 (52.4%)	19 (48.7%)	0.921*
None/low visibility on low-energy images	5 (23.8%)	16 (41.0%)	
Moderate visibility on low-energy images	2 (9.5%)	7 (17.9%)	
High visibility on low-energy images	14 (66.7%)	16 (41.0%)	0.166*
Persistent enhancement	10 (47.6%)	29 (74.4%)	
Plateau enhancement	9 (42.9%)	9 (23.1%)	
Washout enhancement	2 (9.5%)	1 (2.6%)	0.100*
Axillary lymphadenopathy	11 (52.4%)	17 (43.6%)	0.593
Skin thickening	2 (9.5%)	18 (46.2%)	**0.004**
Nipple retraction	4 (19.0%)	13 (33.3%)	0.369
Skin retraction	2 (9.5%)	8 (20.5%)	0.470
Fistula formation	1 (4.8%)	8 (20.5%)	0.142

Data are presented as median (interquartile range) or n (%). Statistically significant *P* values are shown in bold. Patients demonstrating both a mass lesion and non-mass enhancement (n = 10) were excluded from this subgroup analysis to allow comparison of mutually exclusive imaging phenotypes. **P* values calculated for the overall distribution of the corresponding categorical variable. NME, non-mass enhancement.

Table 3. Frequency of malignancy-mimicking imaging findings (n = 70)

Imaging feature	n (%)
Moderate or high conspicuity on recombined images	44 (62.9)
Plateau or washout temporal enhancement pattern	22 (31.4)
Irregular mass shape	7 (10.0)
Indistinct or spiculated mass margin	8 (11.4)
Heterogeneous enhancement	31 (44.3)
Rim enhancement	16 (22.9)
Segmental or linear non-mass enhancement distribution	18 (25.7)
Clumped enhancement	5 (7.1)
Skin thickening	23 (32.9)
Skin retraction	11 (15.7)
Nipple retraction	20 (28.6)
Axillary lymphadenopathy	33 (47.1)

Data are presented as *n* (%), calculated for the entire study cohort (n = 70).

Table 4. Cumulative distribution of the malignancy-mimicking feature score

Cumulative MMFS level	Patients, n (%)
≥ 1 feature	70 (100.0)
≥ 2 features	63 (90.0)
≥ 3 features	46 (65.7)
≥ 4 features	28 (40)
≥ 5 features	19 (27.1)
≥ 6 features	7 (10.0)
≥ 7 features	4 (5.7)
≥ 8 features	1 (1.4)

The MMFS represents an exploratory descriptive measure of the cumulative burden of malignancy-mimicking contrast-enhanced mammography features and is not intended to represent a diagnostic or discriminatory scoring system. MMFS, malignancy-mimicking feature score.

groups are needed to determine whether individual CEM features or their cumulative burden can contribute to the differentiation of IGM from breast malignancy.

Footnotes

Conflict of interest disclosure

The authors declared no conflicts of interest.

References

1. Kessler E, Wolloch Y. Granulomatous mastitis: a lesion clinically simulating carcinoma. *Am J Clin Pathol.* 1972;58(6):642-646. [Crossref]
2. Ozturk M, Mavili E, Kahriman G, Akcan AC, Ozturk F. Granulomatous mastitis: radiological findings. *Acta Radiol.* 2007;48(2):150-155. [Crossref]
3. Bani-Hani KE, Yaghan RJ, Matalka II, Shatnawi NJ. Idiopathic granulomatous mastitis: time to avoid unnecessary mastectomies. *Breast J.* 2004;10(4):318-322. [Crossref]
4. Altintoprak F, Kivilcim T, Ozkan OV. Aetiology of idiopathic granulomatous mastitis. *World J Clin Cases.* 2014;2(12):852-858. [Crossref]
5. Freeman CM, Xia BT, Wilson GC, et al. Idiopathic granulomatous mastitis: a diagnostic and therapeutic challenge. *Am J Surg.* 2017;214(4):701-706. [Crossref]
6. Dilaveri C, Degnim A, Lee C, DeSimone D, Moldoveanu D, Ghosh K. Idiopathic granulomatous mastitis. *Breast J.* 2024;2024:6693720. [Crossref]
7. Boufettal H, Essodegui F, Noun M, Hermas S, Samouh N. Idiopathic granulomatous mastitis: a report of twenty cases. *Diagn Interv Imaging.* 2012;93(7-8):586-596. [Crossref]
8. Yildiz S, Aralasmak A, Kadioglu H, et al. Radiologic findings of idiopathic granulomatous mastitis. *Med Ultrason.* 2015;17(1):39-44. [Crossref]
9. Jochelson MS, Lobbes MBI. Contrast-enhanced mammography: state of the art. *Radiology.* 2021;299(1):36-48. [Crossref]
10. Lobbes MB, Smidt ML, Houwers J, Tjan-Heijnen VC, Wildberger JE. Contrast enhanced mammography: techniques, current results, and potential indications. *Clin Radiol.* 2013;68(9):935-944. [Crossref]
11. Patel BK, Lobbes MBI, Lewin J. Contrast enhanced spectral mammography: a review. *Semin Ultrasound CT MR.* 2018;39(1):70-79. [Crossref]
12. Krawczyk N, Kühn T, Ditsch N, et al. Idiopathic granulomatous mastitis as a benign condition mimicking inflammatory breast cancer: current status, knowledge gaps and rationale for the GRAMAREG study (EUBREAST-15). *Cancers (Basel).* 2024;16(19):3387. [Crossref]
13. Kataria N, Parker EU, Kilgore MR, Scheel JR. Idiopathic granulomatous mastitis of the breast: radiologic-pathologic correlation. *J Breast Imaging.* 2021;3(1):87-92. [Crossref]
14. Pluguez-Turull CW, Nanyes JE, Quintero CJ, et al. Idiopathic granulomatous mastitis: manifestations at multimodality imaging and pitfalls. *Radiographics.* 2018;38(2):330-356. [Crossref]
15. Fazzio RT, Shah SS, Sandhu NP, Glazebrook KN. Idiopathic granulomatous mastitis: imaging update and review. *Insights Imaging.* 2016;7(4):531-539. [Crossref]
16. Sripathi S, Ayachit A, Bala A, Kadavigere R, Kumar S. Idiopathic granulomatous mastitis: a diagnostic dilemma for the breast radiologist. *Insights Imaging.* 2016;7(4):523-529. [Crossref]
17. Dursun M, Yilmaz S, Yahyayev A, et al. Multimodality imaging features of idiopathic granulomatous mastitis: outcome of 12 years of experience. *Radiol Med.* 2012;117(4):529-538. [Crossref]
18. Soylu Boy FN, Esen Icten G, Kayadibi Y, Tasdelen I, Alver D. Idiopathic granulomatous mastitis or breast cancer? A comparative MRI study in patients presenting with non-mass enhan cement. *Diagnostics (Basel).* 2023;13(8):1475. [Crossref]
19. Erkoc N, Karlı EH, Tokoçin M, Gülkaç BÖ, Kalpakoğlu ER, Cimilli AT. Breast MRI features of idiopathic granulomatous mastitis and invasive breast carcinoma: a single-center comparative study. *Clin Imaging.* 2026;134:110798. [Crossref]
20. Aslan H, Pourbagher A, Colakoglu T. Idiopathic granulomatous mastitis: magnetic resonance imaging findings with diffusion MRI. *Acta Radiol.* 2016;57(7):796-801. [Crossref]
21. Zhao Q, Xie T, Fu C, et al. Differentiation between idiopathic granulomatous mastitis and invasive breast carcinoma, both presenting with non-mass enhancement without rim-enhanced masses: the value of whole-lesion histogram and texture analysis using apparent diffusion coefficient. *Eur J Radiol.* 2020;123:108782. [Crossref]
22. Mohamed Kamal R, Hussien Helal M, Wessam R, Mahmoud Mansour S, Godda I, Alieldin N. Contrast-enhanced spectral mammography: impact of the qualitative morphology descriptors on the diagnosis of breast lesions. *Eur J Radiol.* 2015;84(6):1049-1055. [Crossref]
23. Al-Khawari HA, Al-Manfouhi HA, Madda JP, Kovacs A, Sheikh M, Roberts O. Radiologic features of granulomatous mastitis. *Breast J.* 2011;17(6):645-650. [Crossref]
24. Yang ML, Bhimani C, Roth R, Germaine P. Contrast enhanced mammography: focus on frequently encountered benign and malignant diagnoses. *Cancer Imaging.* 2023;23(1):10. [Crossref]
25. Tohamey YM, Youssry SW, Abd El Aziz AI. Interpretation of patterns of enhancement on contrast-enhanced spectral mammography: an approach to a standardized scheme. *Egypt J Radiol Nucl Med.* 2018;49(3):854-868. [Crossref]
26. Kornecki A. Current status of contrast enhanced mammography: a comprehensive review. *Can Assoc Radiol J.* 2022;73(1):141-156. [Crossref]
27. Dromain C, Balleyguier C, Adler G, Garbay JR, Delaloge S. Contrast-enhanced digital mammography. *Eur J Radiol.* 2009;69(1):34-42. [Crossref]
28. Dromain C, Balleyguier C, Muller S, et al. Evaluation of tumor angiogenesis of breast carcinoma using contrast-enhanced digital mammography. *AJR Am J Roentgenol.* 2006;187(5):W528-W537. [Crossref]
29. Partridge SC, Rahbar H, Murthy R, et al. Improved diagnostic accuracy of breast MRI through combined apparent diffusion coefficients and dynamic contrast-enhanced kinetics. *Magn Reson Med.* 2011;65(6):1759-1767. [Crossref]
30. Kuhl CK, Mielcareck P, Klaschik S, et al. Dynamic breast MR imaging: are signal intensity time course data useful for differential diagnosis of enhancing lesions? *Radiology.* 1999;211(1):101-110. [Crossref]
31. Nori J, Kaur M, editors. Contrast-enhanced digital mammography (CEDM). Cham: Springer International Publishing; 2018. [Crossref]